

Quasiparticle band structure based on a generalized Kohn-Sham scheme

F. Fuchs,* J. Furthmüller, and F. Bechstedt

Institut für Festkörpertheorie und -optik, Friedrich-Schiller-Universität, Max-Wien-Platz 1, D 07743 Jena, Germany

M. Shishkin, G. Kresse

Institut für Materialphysik and Center for Computational Materials Science, Universität Wien, A 1090 Wien, Austria

(Dated: December 2, 2024)

We present the first comparative full-potential study of generalized Kohn-Sham schemes (gKS) with explicit focus on their suitability as starting point for the calculation of quasiparticle (QP) states. We compare G_0W_0 quasiparticle bandstructures calculated upon LDA, sX, HSE03, PBE0, and HF functionals for exchange and correlation (XC) for several semiconductors and insulators. It is shown, that the QP energies resulting from a perturbative treatment of the GW self-energy are, with the exception of HF, rather independent of the start functional. We especially suggest the use of a gKS scheme as a starting point for solids with a wrong energetic ordering of the bands within local and semilocal approximations for XC and such with shallow d bands.

PACS numbers: 71.15.Mb, 71.15.Qe, 71.20.Nr

Density Functional Theory (DFT) has become the most successful method for condensed matter calculations. This success is largely due to the simplicity of the exchange and correlation (XC) energy in the local density (LDA) or generalized gradient (GGA) approximation. However, the underlying Kohn-Sham (KS) formalism fails in the prediction of electronic excitation energies of semiconductors and insulators [1]. A significant step forward to correct excitation energies was achieved when the first *ab initio* calculations of quasiparticle (QP) states were performed [2, 3]. In general, they are based on Hedin's GW approximation (GWA) for the self-energy [4] and a perturbative treatment of the difference to the XC potential used in the KS equation. The central quantity is the dynamically screened Coulomb potential W which characterizes the reaction of the electronic system after excitation. For many nonmetals, such as the semiconductor silicon (Si), the method works well with an accuracy of 0.1–0.3 eV for their QP gaps [1], if the Green's function G is described by one pole at the KS (i.e., G_0), or better, at the QP energy. However, for systems with a wrong energetic ordering of the KS bands first-order perturbation theory is not applicable [5]. Examples are semiconductors with a negative fundamental gap in DFT-LDA or -GGA, e.g. InN [6] (and references therein), or with too shallow d -bands, e.g. ZnO [7].

Besides the KS approach itself, the origin of the band gap problem is related to the semi-local approximation (LDA/GGA) for XC, which introduces an unphysical self-interaction and lacks a derivative discontinuity [8, 9]. These deficiencies can be partially overcome using self-interaction-free exact exchange (EXX) potentials [10], which are special realizations of an optimized effective potential (OEP) [7]. A, by conception, different way to address the band gap problem is the use of a generalized Kohn-Sham (gKS) scheme, which means starting from a scheme with a spatially non-local XC potential [11]. In this framework the screened-exchange (sX) approximation uses a statically screened Coulomb kernel instead of the bare kernel in the Hartree-Fock (HF) exchange [11] and, with it, resembles the screened-exchange (SEX)

contribution to the XC self-energy in the GWA [3, 4]. Other hybrid functionals such as those following the suggestions of Adamo and Barone (PBE0) [12] or Heyd, Scuseria, and Ernzerhof (HSE03) [13] combine parts of bare or screened exchange with an explicit density functional. The gKS eigenvalues are usually in much better agreement with the experiment than the LDA/GGA ones. Therefore the gKS solutions are supposed to be superior starting points for a QP correction, since first-order perturbation theory should be justified. Hence the replacement of G by G_0 calculated from solutions of a gKS scheme may be interpreted as a first step towards a self-consistent determination of the self-energy operator [14, 15].

In this Letter we report a systematic study of QP energies calculated from G_0W_0 corrections to the results of gKS schemes. In the first part of this letter we evaluate the performance of different gKS starting points for Si, InN, and ZnO using the functionals sX, HSE03, PBE0, and HF. The results are compared to those of the standard KS approach based on an LDA functional. In the second part QP gaps are calculated for a benchmark set of 14 non-metals utilizing the HSE03 starting point, which was found to be one of the best performing approaches in the first part. The results are compared to those of based on a GGA starting point.

In first-order perturbation theory the measurable QP excitation energies ($\varepsilon_\lambda^{\text{QP}}$) are related to the gKS eigenvalues ($\varepsilon_\lambda^{\text{gKS}}$) through

$$\varepsilon_\lambda^{\text{QP}} = \varepsilon_\lambda^{\text{gKS}} + Z_\lambda \text{Re} \langle \Psi_\lambda^{\text{gKS}} | \Sigma(\varepsilon_\lambda^{\text{gKS}}) - V_{XC}^{\text{gKS}} | \Psi_\lambda^{\text{gKS}} \rangle, \quad (1)$$

where Z_λ is the renormalization factor given by

$$Z_\lambda = (1 - \text{Re} \langle \Psi_\lambda^{\text{gKS}} | \frac{\delta}{\delta \omega} \Sigma(\omega) \Big|_{\varepsilon_\lambda^{\text{gKS}}} | \Psi_\lambda^{\text{gKS}} \rangle). \quad (2)$$

In the sense of a first iteration this approach is usually denoted by G_0W_0 [1, 14]. The perturbation operator $\Sigma - V_{XC}$ is given as the difference of the *GW* self-energy and the non-local XC potential V_{XC}^{gKS} used in the gKS equation. Its smallness suggests that non-diagonal elements and hence an update

of the QP eigenfunctions can be neglected [5]. The diagonal elements $\Delta_{\lambda\lambda}(\varepsilon) = Z_{\lambda} \text{Re} \langle \Psi_{\lambda}^{gKS} | \Sigma(\varepsilon) - V_{XC}^{gKS} | \Psi_{\lambda}^{gKS} \rangle$ define the QP shift for a certain gKS state. The advantage of the relation (1) is to avoid unphysical double poles in the resulting QP Green's function.

The calculations were performed at the experimental lattice constants. We use the projector augmented-wave (PAW) method as implemented in the Vienna *Ab initio* Simulation Package [16]. For the details of the GW implementation we refer to Ref. [17]. The GW calculations were carried out using a total number of 150 bands for all materials. For the Brillouin-zone integrations $8 \times 8 \times 8$ Monkhorst-Pack (MP) k -point meshes, shifted to include the Γ point, were used, except in case of ZnO(LDA) and InN(sX,HSE03) where the k -point convergence of W was found to be critical for meshes containing Γ . There, for W , $8 \times 8 \times 8$ k -points avoiding Γ were used to sample the BZ.

One problem of the presence of shallow d -levels is the strong core-valence XC interaction [14, 18]. It can be estimated within the LDA or HF approximation, where the latter one is expected to be more reliable, since the GW self-energy approaches the bare Fock exchange operator in the short wave-length regime (i.e., at large electron binding energies). Here we use the HF approximation for core-valence in all GW and the gKS calculations reported in Table II and III. In all LDA/GGA and the HSE03 calculations in Table IV we treat the core-valence XC on the gKS level to facilitate comparison with available literature.

In the actual implementation of the gKS schemes we split the gKS XC energy into the form:

$$E_{XC}^{gKS} = E_{XC}^{LDA} + \alpha \left[E_X^{sr}(\mu) - E_X^{LDA,sr}(\mu) \right], \quad (3)$$

i.e., a short range non-local exchange term is added and treated exactly resulting in a non-local (screened) exchange potential. The superscript *LDA* indicates that the respective quantity is evaluated in some (quasi)local approximation, while E_X^{sr} corresponds to one of the (screened) Coulomb kernels given in Table I. The weight α of the short range part and the inverse screening length μ are also listed in this table. For simplicity, in the case of sX, the inverse screening length μ corresponding to the Thomas-Fermi wavevector was chosen materials independent $k_{TF} = 1.55 \text{ \AA}^{-1}$. The results of the gKS calculations are summarized in Table II together with experimental results. We notice an increase of the computed gaps when going from the local density approximation

TABLE I: Parameters of the gKS exchange functionals used.

Functional	α	sr Coulomb kernel	$\mu [\text{\AA}^{-1}]$
LDA	0.00	$1/ \mathbf{x} $	-
sX	1.00	$\exp(-\mu \mathbf{x})/ \mathbf{x} $	1.55
HSE03	0.25	$\text{erfc}(\mu \mathbf{x})/ \mathbf{x} $	0.3
PBE0	0.25	$1/ \mathbf{x} $	-
HF	1.00	$1/ \mathbf{x} $	-

TABLE II: Direct and indirect generalized KS band gaps $E_{g(d,i)}^{gKS}$ and average d -band binding energies E_d^{gKS} calculated for cubic Si, ZnO, and InN. Experimental values are from data collections in Refs. [6, 19, 20, 21, 23]. In the case of InN and ZnO they refer to the wurtzite polytype. All values are given in eV.

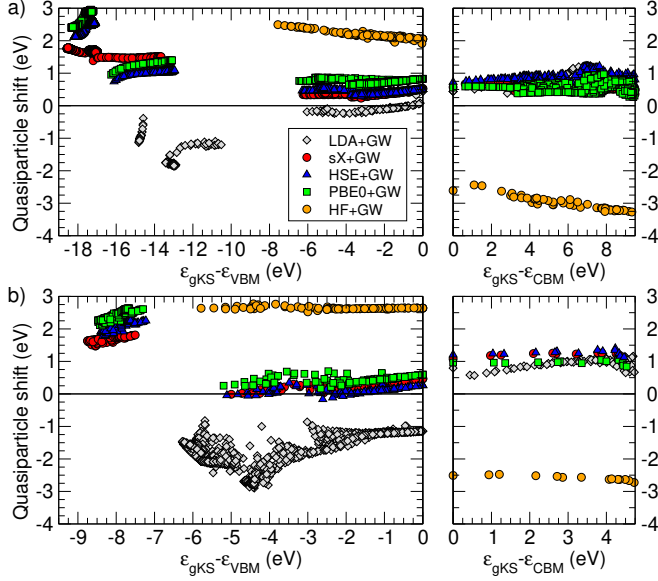
	Energy	LDA	sX	HSE03	PBE0	HF	Exp.
Si	$E_{g,i}^{gKS}$	0.51	0.96	0.99	1.83	6.63	1.17
	$E_{g,d}^{gKS}$	2.53	3.23	3.16	4.01	9.13	3.4
ZnO	E_g^{gKS}	0.6	2.94	2.36	3.31	11.03	3.44
	E_d^{gKS}	5.5	8.2	7.9	8.0	9.5	7.0-8.8
InN	E_g^{gKS}	-0.34	0.53	0.38	1.16	7.20	0.7
	E_d^{gKS}	13.0	17.1	17.2	17.4	18.6	16.0-16.9

to a truly non-local XC functional. This can be attributed to the reduction of the spurious self-interaction found in LDA, the inclusion of a derivative discontinuity in the XC functional [8, 9, 11], and the – in comparison to LDA – enhanced core-valence exchange. Furthermore, for direct gaps we observe the tendency to increase from LDA over HSE03, sX and PBE0 to the HF values. For ZnO and InN, a significant increase of the d band binding energies with respect to the LDA occurs, improving the results towards the experiment. Moreover, these energies are found to vary only little with the gKS functional (apart from HF).

In comparison to experiment the gKS functionals, with exception of HF, generally perform better than standard DFT-LDA for gaps as well as binding energies of the d electrons. There is another important fact to note for InN. All gKS functionals are found to yield the correct ordering of the $\Gamma_{1,c}$ and $\Gamma_{15,v}$ states at the zone center, in contrast to LDA findings [6] which give a negative sp gap. This is essential for the QP description, since a correct energetic ordering of the single-particle states is an inevitable prerequisite for a perturbative treatment of the GW corrections [1, 15]. The fundamental gap of ZnO is considerably opened.

For InN and ZnO the resulting QP shifts (1) are plotted in Fig. 1 versus the gKS eigenenergies. For InN [Fig. 1(a)] the QP shifts for the upper valence bands and the conduction bands show a rather weak dispersion with the eigenstate. They may be approximated by scissor operators for occupied and empty states whose absolute values depend on the used gKS functional LDA, sX, HSE03, or PBE0. Only for the lowest In4d- and N2s-derived bands at gKS energies below -10 eV the QP shifts show a noticeable dispersion. This is most pronounced in the LDA case and reduces significantly upon the use of a gKS functional. Interestingly, the sX starting point leads to the weakest variation of the QP shifts in all energy regimes considered. This is attributed to the conceptual proximity of sX to the SEX term in the GW self-energy which dominates the state dependence of the QP shifts. The findings for ZnO (Fig. 1b) are similar. However, since the Zn3d states are bound much weaker, the effect of the pd repulsion is stronger than in InN resulting in a stronger influence of the

FIG. 1: (Color online) Quasiparticle shifts versus gKS eigenvalues for InN (a) and ZnO (b). The valence-band maximum (VBM) and the conduction-band minimum (CBM) are taken as energy zeros for occupied and empty states, respectively. Results for five different starting gKS band structures are shown



d electrons on the uppermost occupied states and hence the corresponding QP shifts.

It is worthwhile to analyse the QP shifts in Fig. 1. First, for the occupied states there exists an offset between the LDA and the sX/HSE03/PBE0 shifts, which renders the LDA QP shifts mainly negative. This is predominately caused by the core-valence XC contribution to the QP shifts, which is nonzero only in the case of LDA. The effect scales with the localisation of the states, which is clearly visible for the *d* states and the more negative values for ZnO in comparison to InN. Due to this the effect is largely reduced for the unoccupied states, and in the case of silicon (not shown here). Therefore, the QP corrections for empty states are (except of HF) rather independent of the starting fundamental. Second, compared to the LDA the absolute QP shifts are in general not smaller for a gKS starting point. For the topmost valence bands and the conduction bands the absolute shifts are in the order of 1 eV. Third, in the extreme limit of the HF starting point the QP shifts are given by the correlation self-energy Σ_C scaled with the dynamical renormalization factor and consequently undergo the sign-change of Σ_C at the Fermi level.

Table III shows the results of the G_0W_0 calculations for gaps, band widths, and *d*-electron binding energies. In contrast to the LDA or gKS energies, the QP energies shown in Table III should have a physical meaning as measurable quantities and thus can be compared directly to the experimental gap-values. For silicon the QP gaps calculated upon the LDA, sX or HSE03 starting point bracket the experimental values, closely, with a maximum deviation of 0.2 eV. The LDA+ G_0W_0 values thereby slightly underestimate the gaps. In fact, this is a realisation of a general trend of gap-underestimation in the

TABLE III: Direct (d) and indirect (i) G_0W_0 QP band gaps and average *d*-band binding energies calculated upon the respective gKS bandstructures for Si, ZnO, and InN. All values are given in eV. Experimental results are given for comparison.

	Energy	LDA	sX	HSE03	PBE0	HF	Exp.
Si	$E_{g,i}^{QP}$	1.06	1.30	1.30	1.53	2.99	1.17
	$E_{g,d}^{QP}$	3.17	3.49	3.47	3.72	5.26	3.4
ZnO	E_g^{QP}	2.54	3.55	3.30	3.68	5.88	3.44
	E_d^{QP}	6.2	7.0	6.1	6.2	7.8	7.0-8.8
InN	E_g^{QP}	0.00	0.57	0.59	0.90	2.54	0.7
	E_d^{QP}	15.0	16.0	15.2	15.3	17.0	16.0-16.9

LDA/GGA+ G_0W_0 approach using full-potential methods recently established by different groups [15, 23]. For the gKS starting points, the calculated gaps are larger than the experimental ones. In more detail starting from sX or HSE03 is found to yield virtually identical results, very close to the experiment. The PBE0+ G_0W_0 approach overestimates the gaps significantly just like the HF+ G_0W_0 approach, for which however the deviations are more extreme. In the latter case this is the consequence a break-down of the perturbative QP treatment in (1), due to too large differences between ϵ_{λ}^{QP} and ϵ_{λ}^{HF} . For the PBE0 starting point, however, the deviations are of different origin. Evaluating the RPA-dielectric constants suggests an underscreening for the PBE0 starting point, which in turn causes the overestimation of the gaps. For ZnO and InN the presence of shallow *d*-electrons influences the position of the VBM and therefore the fundamental gaps by the *pd* repulsion [18]. Since the LDA significantly underbinds the *d*-electrons, due the spuriously contained self-interactions, it in turn increases the *pd* repulsion and thereby additionally reduces the gap. However not just the electronic structure is questionable, but also the VBM wavefunctions are affected resulting in an unreasonably high *d* admixture. Together with the unusually drastic gap underestimation, a successfull LDA+ G_0W_0 treatment is hampered. Although the trends just discussed for Si still hold, the actual benefit of a gKS starting point become more apparent for ZnO and InN. Contrary to the LDA, the gKS starting points reproduce the correct ordering of gap states and yield, at least in the case of sX and HSE03, more meaningful dielectric constants. Taken into account, that the experimental gaps given in Table III refer to the wurzite structure for ZnO and InN, the agreement between them and the sX+ G_0W_0 or HSE03+ G_0W_0 results is fair. Compared to the gaps, the *d* band binding energies calculated for InN and ZnO show a stronger variation with the starting XC functional. Nevertheless, the agreement of the calculated values with experimental ones (Table III) is good for InN. For ZnO with more shallow *d* levels the picture is less clear, although, here the comparison with experiment is also hampered by the remarkable scatter in the measured values. In any case, the better treatment of exchange and correlation due to the gKS starting functionals improves the predictive power

TABLE IV: Gaps calculated in DFT-GGA[22], GGA+ G_0W_0 , HSE03 and HSE03+ G_0W_0 . Experimental data (gaps, lattice constants) for references given in [23]. The calculated values spin-orbit coupling (SO), already included in the gaps, are given in the last column. For the gKS calculations the core-valence was treated on the GGA and HSE03 level respectively, as opposed to Tab. III. Also reported is the mean absolute relative error (MARE).

	GGA[22]	G_0W_0	HSE03	G_0W_0	$E_g^{\text{exp.}}$	a [Å]	SO
Si	0.62	1.12	1.00	1.29	1.17	5.430	
GaAs	0.49	1.29	0.89	1.57	1.52	5.648	0.10
SiC	1.35	2.27	2.08	2.59	2.40	4.350	
CdS	1.14	2.06	1.71	2.43	2.42	5.832	0.02
AlP	1.57	2.44	2.05	2.64	2.45	5.451	
GaN	1.62	2.88	2.66	3.41	3.20	4.520	0.00
ZnO	0.67	2.43	2.06	3.25	3.44	4.580	0.01
ZnS	2.07	3.47	2.84	3.83	3.91	5.420	0.02
C	4.12	5.50	5.12	5.86	5.48	3.567	
BN	4.45	6.10	5.57	6.53	6.1-6.4	3.615	
MgO	4.76	7.25	6.20	7.96	7.83	4.213	
LiF	9.20	13.27	11.05	14.07	14.20	4.010	
Ar	8.69	13.28	9.68	13.62	14.20	5.260	
Ne	11.61	19.59	13.96	20.31	21.70	4.430	
MARE	45 %	9%	23%	5%			

for the energy positions of the semicore d -bands although it is somewhat reduced compared to the accuracy of the gap determination.

In order to facilitate a gauge of a gKS starting point against a (semi)local one, we calculated the G_0W_0 QP gaps starting from GGA and HSE03 for 14 materials ranging from small-gap semiconductors to insulators. The results are shown in Table. IV. For materials comprising shallow d bands the HSE03+ G_0W_0 approach performs significantly better than GGA+ G_0W_0 , whereas for the rest of the materials the deviations from experiment are comparable for both approaches, with the overall error being almost halved in the HSE03+ G_0W_0 approach. Usually HSE03+ G_0W_0 overestimates the band gaps, slightly, whereas for ZnO, ZnS, LiF, Ar and Ne, the band gaps remain underestimated compared to experiment, which we attribute to the prevailing inaccuracy of perturbation theory: these systems are exchange dominated (static dielectric constant smaller 4), and the HSE03 error is larger than 20 % and thus not yet sufficiently small for a perturbative treatment.

In conclusion, we have presented QP calculations starting from gKS schemes with a variety of XC functionals LDA, sX, HSE03, PBE0, and HF for fifteen materials ranging from small gap semiconductors to insulators. We identified the gKS schemes that take into account a screened exchange potential or parts of it (sX, HSE03) to give rise to eigenvalues close to the experimental excitation energies. The resulting G_0W_0 corrections are found to yield QP energies almost independent of the actual starting functional and compare well with the experiment (especially for gaps). In addition a benchmark of the HSE03+ G_0W_0 approach for the fundamental gaps of various materials was provided, yielding an average mean absolute error of only 5 % (compared to 9 % using GGA+ G_0W_0). We

identified the tendency of the HSE03+ G_0W_0 approach to overestimate the gaps, except for exchange dominated systems. Vast improvements over the LDA/GGA were found for materials with shallow d bands, where the gKS starting points predict the correct ordering of gap-states and more meaningful screening properties. The use of gKS functions as starting points for GW calculations instead of LDA or GGA therefore seems to be a way to avoid the self-consistent inclusion of nondiagonal elements of the self-energy operator [24] and, hence, should allow QP calculations for complex systems, circumventing the methodological complications and the numerical effort of self-consistent GW calculations [15, 24].

Financial support by the Deutsche Forschungsgemeinschaft (Project No. Be 1346/18-1) and the European Community in the framework of the network of excellence NANOQUANTA (Contract No. NMP4-CT-2004-500198) and the Austrian FWF (SFB25 IR-ON, START-Y218) is gratefully acknowledged.

* Electronic address: fuchs@ifto.physik.uni-jena.de

- [1] W. Aulbur, L. Jönsson, and J. Wilkins, Solid State Phys. **54**, 1 (2000).
- [2] R. W. Godby, M. Schlüter, and L. J. Sham, Phys. Rev. Lett. **56**, 2415 (1986).
- [3] M. S. Hybertsen and S. G. Louie, Phys. Rev. Lett. **55**, 1418 (1985).
- [4] L. Hedin, Phys. Rev. **139**, A796 (1965).
- [5] O. Pulci, F. Bechstedt, G. Onida, R. Del Sole, and L. Reining, Phys. Rev. B **60**, 16758 (1999).
- [6] J. Furthmüller, P. H. Hahn, F. Fuchs, and F. Bechstedt, Phys. Rev. B **72**, 205106 (2005).
- [7] P. Rinke, A. Qteish, Neugebauer, C. Freysoldt, and M. Scheffler, New J. Phys. **7**, 126 (2005).
- [8] J. P. Perdew and M. Levy, Phys. Rev. Lett. **51**, 1884 (1983).
- [9] L. J. Sham and M. Schlüter, Phys. Rev. Lett. **51**, 1888 (1983).
- [10] M. Städele, J. A. Majewski, P. Vogl, and A. Görling, Phys. Rev. Lett. **79**, 2089 (1997).
- [11] A. Seidl, A. Görling, P. Vogl, J. A. Majewski, and M. Levy, Phys. Rev. B **53**, 3764 (1996).
- [12] C. Adamo and V. Barone, J. Chem. Phys. **110**, 6158 (1999).
- [13] J. Heyd, G. E. Scuseria, and M. Ernzerhof, J. Chem. Phys. **118**, 8207 (2003).
- [14] W. Ku and A. G. Eguiluz, Phys. Rev. Lett. **89**, 126401 (2002).
- [15] T. Kotani and M. van Schilfgaarde, Solid State Commun. **121**, 461 (2002).
- [16] G. Kresse and J. Furthmüller, Comp. Mat. Science **6**, 15 (1996).
- [17] M. Shishkin and G. Kresse, Phys. Rev. B **74**, 035101 (2006).
- [18] S. Sharma, J. K. Dewhurst, and C. Ambrosch-Draxl, Phys. Rev. Lett. **95**, 136402 (2005).
- [19] L. F. J. Piper *et al.*, Phys. Rev. B **72**, 245319 (2005).
- [20] L. Ley *et al.*, Phys. Rev. B **9**, 600 (1974).
- [21] R. Girard *et al.*, Surface Science **373**, 409 (1997).
- [22] J. P. Perdew, K. Burke, and M. Ernzerhof, Phys. Rev. Lett. **77**, 3865 (1996).
- [23] M. Shishkin and G. Kresse, Phys. Rev. B submitted.
- [24] M. van Schilfgaarde, T. Kotani, and S. Faleev, Phys. Rev. Lett. **96**, 226402 (2006).